Phonon scattering in silicon films with thickness of order 100 nm

Y. S. Ju and K. E. Goodson[a)]
Department of Mechanical Engineering, Stanford University, Stanford, California 94305-3030

(Received 26 January 1999; accepted for publication 21 March 1999)

Although progress has been made in the *ab initio* simulation of lattice dynamics in semiconducting crystals, information about the relaxation of nonequilibrium lattice vibrations remains incomplete. This work studies the relaxation times of room-temperature thermal phonons through measurements of thermal conduction along monocrystalline silicon films of thickness down to 74 nm. A repetitive oxidation and etching process ensures that the purity and crystalline quality of the films are comparable with those of bulk samples. Phonon-interface scattering reduces the thermal conductivity by up to 50% at room temperature. The data indicate that the effective mean-free path of the dominant phonons at room temperature is close to 300 nm and thus much longer than the value of 43 nm predicted when phonon dispersion is neglected. This study indicates that a broad variety of lattice transport characteristics for bulk silicon can be obtained through measurements on carefully prepared silicon nanostructures. The present data are also valuable for the thermal simulation of silicon-on-insulator (SOI) transistors.
[S0003-6951(99)04820-2]

Significant progress has been made in the understanding of the lattice dynamics in silicon as *ab initio* simulations have enabled accurate computation of phonon spectra and the Grüneisen parameters.[1] Information about the relaxation of phonons, however, remains incomplete. This is due partly to the fact that the high-frequency transverse acoustic (TA) phonons in silicon are highly dispersive. Previous theoretical studies[2,3] demonstrated that consideration of the phonon dispersion is critical in modeling the thermal conductivity of silicon near room temperature and above, where phonons with low group velocities become fully excited. There exists significant discrepancy among phonon mean-free paths estimated from the bulk thermal conductivity depending on which phonon branch was taken to dominate heat transport.[4,5]

One way to experimentally observe the mean-free path of phonons is to examine the size effect on the thermal conductivity of thin monocrystalline films, which arises from phonon-boundary scattering. A recent experimental study[6] reported two orders of magnitude reduction in the in-plane thermal conductivity of a 155-nm-thick silicon membrane. Whether such a drastic thermal conductivity drop is due solely to phonon-boundary scattering, however, is unclear. This is partly because the thermal conductivity of crystalline silicon is sensitive to the presence of defects that could be introduced unintentionally during the processing steps, such as substrate back etching. In addition, a recent study[7] suggested that phonon confinement causes the film thermal conductivity to depend very sensitively on the thickness. Other existing measurements were limited to films with thickness close to or over a micrometer and had experimental uncertainties comparable to the observed reduction.[8–10]

The present work experimentally studies the mean-free path of thermal phonons in silicon at room temperature by measuring the in-plane thermal conductivity of monocrystalline thin films. The experimental technique allows measurements on films as thin as 74 nm and eliminates the possible incorporation of unintended defects during substrate etching. As much as 50% reduction from the bulk value is observed. Model predictions accounting for phonon-boundary scattering are made and compared with the data to provide insight into which phonon branch dominates heat transport at elevated temperatures.

The measurement structures are made using commercially available *p*-type (111) silicon-on-insulator (SOI) wafers (SOITEC, France). These wafers are prepared by bonding two oxidized silicon wafers and then removing all but a thin layer of silicon on one side. The silicon layers obtained in this fashion are referred to as BESOI (bond and etch-back silicon-on-insulator) layers, a detailed description of which can be found elsewhere.[11] The BESOI layers are monocrystalline and have no TEM-detectable defects. The thickness of the silicon layer is controlled by repeated thermal oxidation and wet etching. At each oxidation step, the thickness of the silicon-dioxide layer is limited to be less than 30 nm to prevent the development of significant thermal stress. We use a laser interferometer and also a surface profilometer to determine the thicknesses of the layers. The uncertainty in the thickness control procedure, as estimated from comparison between the two independent measurements and the nonuniformity across the wafer, is less than 5%.

The in-plane thermal conductivity of the silicon layers is measured using a technique that has been recently developed by the authors for the characterization of the anisotropic thermal conductivity of thin dielectric films and composite structures. Details of this technique and its application for polyimide films were reported elsewhere.[12] Periodic Joule heating is induced in metal bridges with differing widths that are formed on a film using a photolithography process. The resulting temperature rise in each bridge structure is measured by monitoring the changes in its electrical resistance.

[a)]Electronic mail: goodson@vk.stanford.edu

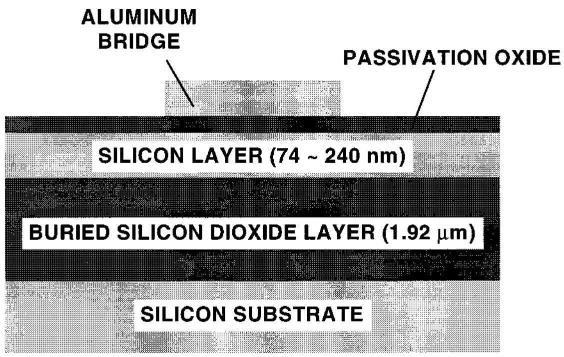

FIG. 1. Cross-sectional view of the thermal conductivity measurement structure employed in the present study.

The measured amplitudes of temperature oscillations are compared with numerical solutions to the heat diffusion equation to extract the in-plane thermal conductivity of the film. Previous studies used a single metal bridge with width much larger than the film thickness to determine the out-of-plane thermal conductivity of dielectric films.[13]

Figure 1 shows a schematic diagram of the cross section of the measurement structure. The buried oxide layer acts as a thermal barrier and forces heat to spread along the silicon film before it reaches the substrate. The thickness of the buried oxide layer is selected such that the spatial extent of lateral heat spreading is much larger than the silicon layer thickness, and hence, the mean-free path of phonons. This is to ensure that the in-plane temperature gradient and the thermal conductivity retain their usual meaning. A thicker buried oxide film would improve accuracy but is difficult to prepare due to limitations in the SOI wafer fabrication process. The metal bridge width is varied between 0.8 and 10 μm, the minimum of which is dictated by the resolution of the optical lithography. The orientation of the bridge structure is such that lateral heat flow along the thin silicon layers occurs predominantly in the $\langle 110 \rangle$ direction. The top silicon-dioxide layer acts as an electrical passivation layer. The thermal conductivity of this passivation layer is taken to be that of a silicon-dioxide film grown on a silicon wafer during the same process run. The latter conductivity is determined using the 3ω technique.[13] The thermal conductivity of the metal layer is determined independently as explained shortly.

The accuracy of the present experimental technique is first verified by measuring the thermal conductivities of aluminum films with thickness comparable to those of the silicon layers. This verification replaces the silicon layer in Fig. 1 with an aluminum film. The aluminum films are sputtered on regular silicon wafers capped with 2-μm-thick low-pressure chemical-vapor deposition silicon-dioxide films. The electronic thermal conductivity is related to the electrical conductivity via the Wiedemann–Franz–Lorenz law, which was shown to be applicable for thin aluminum films of similar thicknesses.[14,15] The thermal conductivity of the aluminum films studied is larger than $100\,\mathrm{W\,m^{-1}\,K^{-1}}$ and the lattice contribution is expected to be negligible. The measured Lorenz numbers agree very well with those of previous studies[14,15] and add confidence in the subsequent measurements on the silicon layers. The main contributors to the experimental uncertainty in the present measurements are the uncertainty in the sample dimensions and the uncertainty in the calibration coefficient of the bridge thermometer.

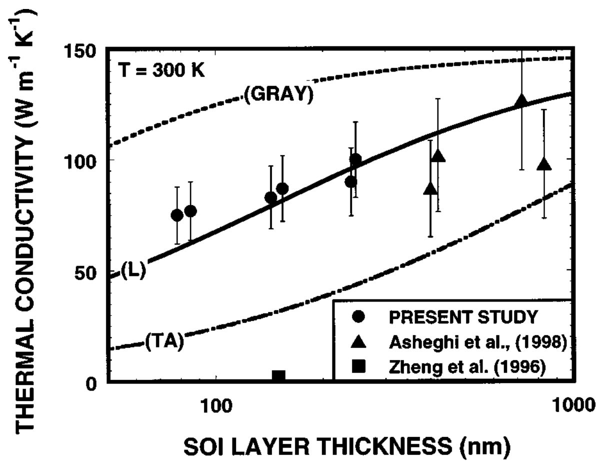

FIG. 2. Measured and predicted in-plane thermal conductivities of thin monocrystalline silicon layers at room temperature. The plot includes data from two previous studies (Ref. 6 and 10).

Figure 2 shows the measured in-plane thermal conductivities of the silicon layers at room temperature. The thermal conductivity is smaller by up to 50% than the bulk value and exhibits relatively weak film thickness dependence. The present data differ substantially from that of a previous study,[6] which used a 155-nm-thick free-standing silicon membrane structure. The discrepancy suggests that defects, which were introduced during the fabrication process, were responsible for the drastic reduction observed in that study. This is consistent with the conclusion of a theoretical study,[16] which examined the effect of dislocations on the in-plane thermal conductivity of thin semiconductor films. Dislocations were considered to be a main source of the anomalous drop in the thermal conductivity of superlattices with long periods.[17] Other existing data[9,10] on thicker silicon films are consistent with the present data. The observed thickness dependence of the thermal conductivity indicates that the size effect due to phonon confinement, which was predicted to result in a substantial thickness dependence,[7] plays a relatively minor role in the thickness range examined here.

Figure 2 also plots the predicted in-plane thermal conductivity of silicon layers. Phonon-boundary scattering is accounted for by using a solution to the Boltzmann transport equation,[18] which relates the mean-free path of carriers in films Λ_{film} to that in bulk samples Λ_{bulk}. Predictions shown in Fig. 2 use Λ_{bulk} that is estimated in three different ways. For the upper-most curve in Fig. 2, phonon dispersion is neglected and all of the phonon modes are assumed to contribute equally to heat transport. A kinetic theory expression, $\Lambda_{\mathrm{bulk}}=3k_{\mathrm{bulk}}/Cv$, yields the mean-free path of 43 nm at room temperature.[5] In the calculation the volumetric heat capacity C is taken to be the bulk value of silicon and v is taken to be the speed of sound. It can be noted that the gray medium approximation, which neglects phonon dispersion, considerably underestimates the size effect.

The other two predictions shown in Fig. 2 assume either longitudinal phonons or high-frequency transverse acoustic phonons as the *sole* heat carriers to gain further insight into the question of which phonon branch is dominant. The ther-

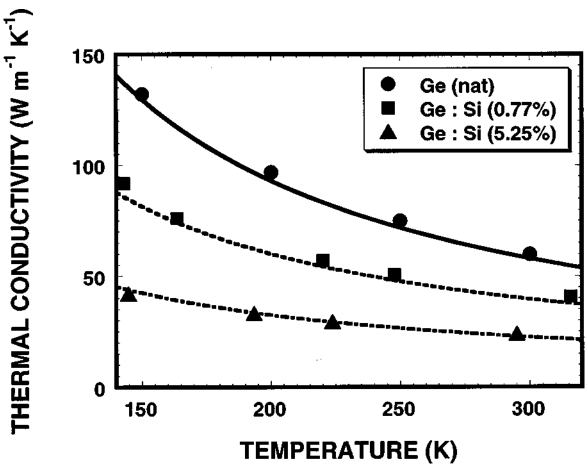

FIG. 3. Model predictions and previous data for the thermal conductivity of germanium crystals. The data for the isotopically enriched sample (Ref. 20), not shown here, are used to fix the model parameter *B*.

mal conductivity integrals of Holland[19] are used to obtain the mean-free path of each branch in bulk samples. For the longitudinal phonons, the phonon–phonon scattering rate is assumed to exhibit a power-law dependence, $\tau^{-1}=B(T)\omega^m$. The exponent m, which governs the frequency dependence of the phonon–phonon scattering rate, is not well known. The present study obtains an estimate of m from the analysis of existing thermal conductivity data of germanium samples with varying concentrations of point defects.[20–22] To the best of our knowledge, no comparable data set exists for silicon. In view of the close similarity between the phonon spectra of silicon and germanium, it is assumed that the same value of m is applicable for silicon. The best fit can be achieved for $m=1.7$, as shown in Fig. 3, which lies between theoretically predicted values of 1 and 2.[19,23] The temperature range considered for germanium, when scaled with respect to the Debye temperature, corresponds to room temperature and above for silicon. Once the exponent m is determined, the coefficient $B(T)$ is obtained by fitting the model to the bulk thermal conductivity data. The frequency dependence of phonon-scattering rates is less important for the TA phonons since they occupy a much narrower frequency range. The experimental data show reasonable agreement with the prediction when the longitudinal phonons are considered to be the dominant heat carriers. The discrepancy can be ascribed partly to the formal exclusion of contributions from other phonon branches in the calculation. A previous theoretical study[2] examined the thermal conductivity of bulk germanium samples and also concluded the dominance of longitudinal phonons.

As a convenient measure of the mean-free path of phonons that dominate heat currents in bulk silicon, an effective mean-free path is estimated. The effective mean-free path is taken here to be the thickness of a film whose thermal conductivity is reduced from the bulk value by a factor given by a solution to the Boltzmann equation with $\Lambda_{\mathrm{bulk}}=d$.[18] Here, d is the film thickness. The experimental data yield the effective mean-free path near 0.3 μm at room temperature, which is in good agreement with a value estimated in connection with the out-of-plane thermal conductivity of silicon–germanium superlattices.[5]

In summary, the present study indirectly observes the mean-free path of phonons in silicon at room temperature by measuring the in-plane thermal conductivity of monocrystalline films with thickness down to 74 nm. A technique is used that avoids the introduction of unintended defects during the sample preparation process. The thermal conductivities of the silicon films are found to be up to 50% lower than the bulk value and suggests the effective phonon mean-free path near 300 nm. Comparison with model calculations suggests that longitudinal phonons are dominant heat carriers in silicon near room temperature.

[1] G.-M. Rinanese, J.-P. Michenaud, and X. Gonze, Phys. Rev. B **53**, 4488 (1996).
[2] K. C. Sood and M. K. Roy, J. Phys.: Condens. Matter **5**, 301 (1993).
[3] M. Omini and A. Sparavigna, Nuovo Cimento D **19**, 1537 (1997).
[4] Y. S. Ju and K. E. Goodson, *Proceedings of the ASME International Mechanical Engineering Congress and Exposition* (ASME, New York, 1997), DSC-Vol. 62, pp. 181–189.
[5] G. Chen Phys. Rev. B **57**, 14958 (1998).
[6] Z. Y. Zheng, S. Z. Li, M. Chen, and K. L. Wang, *Proceedings of the ASME International Mechanical Engineering Congress and Exposition* (ASME, New York, 1996), DSC-Vol. 59, pp. 93–98.
[7] A. Balandin and K. L. Wang, Phys. Rev. B **58**, 1544 (1998).
[8] N. Savvides and H. J. Goldsmid, Phys. Status Solidi B **63**, K89 (1974).
[9] X. Y. Yu, L. Zhang, and G. Chen, Rev. Sci. Instrum. **67**, 2312 (1996).
[10] M. Asheghi, Y. K. Leung, S. S. Wong, and K. E. Goodson, Appl. Phys. Lett. **71**, 1798 (1997).
[11] M. Bruel, Nucl. Instrum. Methods Phys. Res. B **108**, 313 (1996).
[12] Y. S. Ju, K. Kurabayashi, and K. E. Goodson, Thin Solid Films **339**, 160 (1999).
[13] D. G. Cahill, M. Katiyar, and J. R. Abelson, Phys. Rev. B **50**, 6077 (1994).
[14] B. T. Boiko, A. T. Pugachev, and V. M. Bratsychin, Thin Solid Films **17**, 157 (1973).
[15] O. Paul, M. von Arx, and H. Baltes, *Proceedings of the 1995 8th International Conference on Solid-State Sensors and Actuators and Eurosensors IX* (IEEE, Piscataway, NJ, 1995), pp. 178–181.
[16] G. Chen and M. Neagu, Appl. Phys. Lett. **71**, 2761 (1997).
[17] S.-M. Lee, D. G. Cahill, and R. Venkatasubramanian, Appl. Phys. Lett. **70**, 2957 (1997).
[18] E. H. Sondheimer, Adv. Phys. **1**, 1 (1952).
[19] M. G. Holland, Phys. Rev. **132**, 2461 (1963).
[20] T. H. Geballe and G. W. Hull, Phys. Rev. **110**, 773 (1958).
[21] Y. S. Touloukian, R. W. Powell, C. Y. Ho, and P. G. Klemens, *Thermophysical Properties of Matter* (Plenum, New York, 1970).
[22] S. R. Bakhchieva, N. P. Kekelidze, and M. G. Kekua, Phys. Status Solidi A **83**, 139 (1984).
[23] B. H. Armstrong, Phys. Rev. B **32**, 3381 (1985).